Preliminary design of a self-deployable Pulsating Heat Pipe by means of a Shape Memory Alloy actuator

Perna R.[1*], Mameli M.[1], Bucchi F.[2], Frendo F.[2], Filippeschi S.[1]

[1]Department of Energy, Systems Land and Construction Engineering, University of Pisa, Largo L. Lazzarino, Pisa, Italy
[2] Department of Civil and Industrial Engineering, University of Pisa, Largo L. Lazzarino Pisa, Italy

E-mail: roberta.perna@phd.unipi.it

Abstract. The preliminary design of thermally driven self-deployable pulsating heat pipe with Shape Memory Alloy (SMA) actuator is presented. The use of SMA wire allows the passive folding of the heat transfer device: the hot side of the heat exchanger acts as hot source for the SMA deformation. The system consists of a torsion-spring shaped Pulsating Heat Pipe tube portion (Al6063, 1.8 and 2.6 mm inner and outer diameter) and a SMA wire (0.5 mm diameter, closed and open configuration length 165 mm and 172 mm respectively). When the SMA wire is heated up by the hot source, it shortens inducing a moment on the PHP torsion spring that allows the PHP panel to rotate 90 deg.

Keywords: Deployable system, Pulsating Heat Pipe, Shape Memory Alloy actuator.

1. Introduction

The combined use of passive two phase heat exchangers (Heat Pipes) together with the Shape Memory Alloy actuators could provide a robust and reliable solution for the development of thermally driven self-deployable heat transfer devices. The already existing thermal energy source, e.g. on-board electronics for the space field [1] (Fig. 1) or pivotable solar panels in the civil field [2] (Fig. 2), can be exploited to passively act the mechanical mechanisms of movable components. Figure 1 shows a deployable space antenna opened by lastic elements [1] and Figure 2 shows a prototype of passive solar tracker [2].

Due to the absence of a wick structure, the Pulsating Heat Pipe seems the most suitable to be shaped as a torsional spring so as to obtain a deployable structure. Attempts of developing flexible PHPs are already present in the literature. Qu et al. [3] introduced a tubular device with the adiabatic section made of fluoro-rubber material and they characterized it in different foldable configurations. Since polymers may be strongly chemically altered by the space environment conditions [4] and are high permeable to Non Condensing Gases (NCGs), the development of a metallic deployable structure is however preferable for future space applications. Foldable PHP are therefore scarcely investigated.

On the contrary, Shape Memory Alloys are already widely used for the actuation of deployable structures, as they can effectively reduce the actuation complexity if compared to activated systems. The SMA actuators have different shapes: wire, sheet and spring and in most cases, they are usually activated by Joule heating [5]. The use of a SMAs to deploy a PHP represents a challenge since the thermal input

is not uniformly distributed on the actuator as during Joule heating, but it's concentrated only in one side of the actuator while the rest of the alloy is indirectly heated by conduction. It could be critical if the heat transfer device operates in a temperature range close to the temperatures peculiar of the Shape Memory Effect.

The driving idea is to join the PHP with a passive SMA actuator and exploit the hot sources (electronic equipments, batteries, solar collector) that must be thermally controlled by a PHP, to activate the SMA deploying mechanism. This paper presents the proof of concept and a feasibility study of this innovative solution. The feasibility of this solution has been experimentally tested and numerically investigated.

The experimental apparatus presented in this paper is part of the TOPDESS (TwO-phase Passive thermal devices for DEployable Space Systems) project funded by the European Space Agency. The project aims at designing a deployable metallic tubular Pulsating Heat Pipe (PHP) with a Shape Memory Alloy (SMA) actuator for a specific space radiator. The folding of the device is allowed by the torsion spring preload, while the shape memory effect is used for the unfolding.

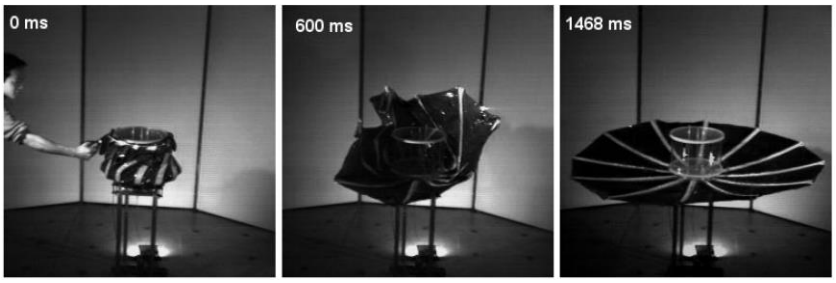

Figure 1. Umbrella like deployable space antenna concept [1].

Figure 2. Prototype of solar tracker [2].

2. The Self-Deployable Pulsating Heat Pipe actuated by Shape Memory Alloy: Design and Concept

The design and the concept of the self-deployable Pulsating Heat Pipe actuated by Shape Memory Alloy (SMA) are shown in Figure 3 and in Figure 4 respectively. The PHP is shaped as torsional spring in the adiabatic section, in a folded configuration (Fig. 3). The evaporator section is mechanically bound to the unmoving part, while the condenser section is bound to the moving section, so that it can be unfold (Fig.4). The SMA wire (Fig.3) is bound to an insulating rigid support and it is thermally connected to the evaporator section (Fig.3). The wire runs through the pulleys without any interference during the PHP spring unfolding. The SMA wire is thermally connected to the hot source so that the heat load simultaneously activates the PHP thermo-fluidics and the SMA wire deformation.

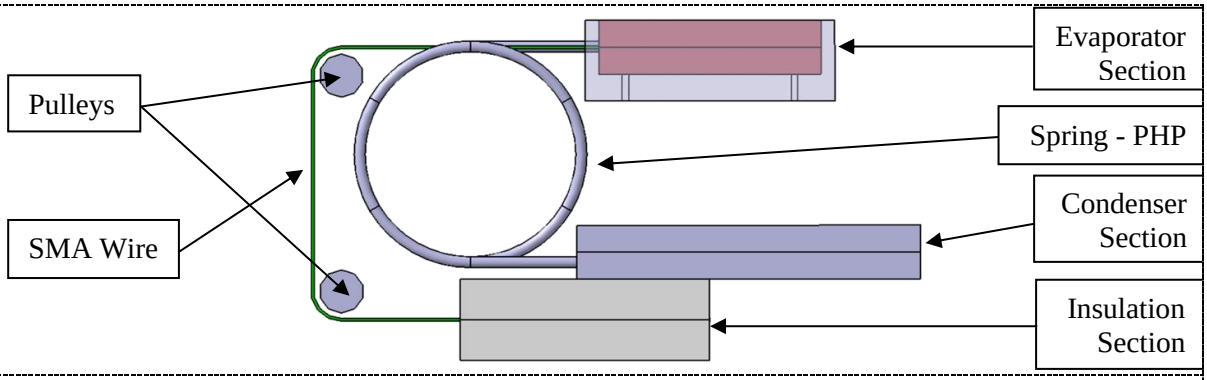

Figure 3. The Self-Deployable Pulsating Heat Pipe actuated by Shape Memory Alloy: Design.

The SMA wire is initially elongated at room temperature before connecting it to the evaporator and insulation sections. Once the heat load ($\dot{Q}$ - Fig.4) is applied, the SMA wire shortens due to Shape Memory Effect (SME), being subject to a phase transformation and applies a force (F_{SMA} - Fig.4) on the moving plate. Then, the SMA wire applies a tension to the insulation section, which induces a moment on the torsion spring which overcomes the spring preload, so that the radiator panel unfolds (θ - Fig.4). The mechanical equilibrium of the mechanism is expressed as follows:

$$F_{SMA} \cdot d_{arm} = M_{PHP}(0) \quad (1)$$

where $M_{PHP}(0)$ is the torsion spring moment at $\theta = 0$ and the spring preload (subsection 3.1), F_{SMA} is the force applied by the SMA wire (subsection 4.1) and $d_{arm}$is the distance between the wire and the PHP mobile straight arm clamp.

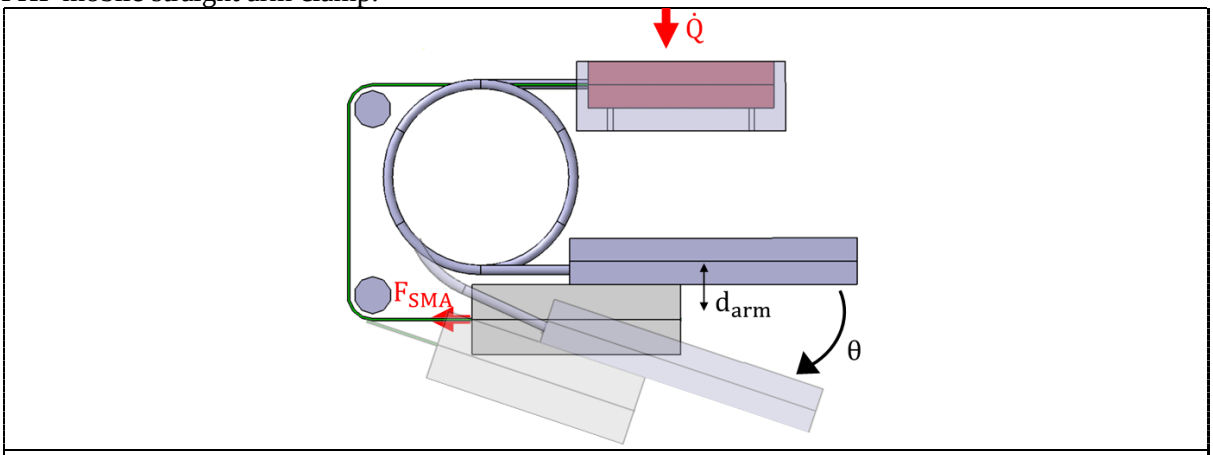

Figure 4. The Self-Deployable Pulsating Heat Pipe actuated by Shape Memory Alloy: Concept.

3. Self-Deployable Pulsating Heat Pipe

3.1. Mechanical Analysis of Spring-shaped Pulsating Heat Pipe

The design of a flexible metallic PHP is linked to two fundamental requirements:

- the internal diameter of the PHP pipe must be smaller than the critical diameter based on the Bond criterion ($d_{in} < d_{Bond}$) to promote a slug/plug flow rate;
- the metallic tube must remain in the elastic deformation range ($\sigma_c^{max} \leq \sigma_y$), so that the torsional effect of the spring can fold and unfold the radiator many times.

The maximum torsional spring coil stress σ_c^{max}, subject to M_{PHP} bending moment, is defined by the following equation:

$$\sigma_c^{max} = K\frac{M_{PHP} \cdot d_{out}}{2 \cdot I} \quad (2)$$

where K is the bending stress correction factor ($K \approx 1$ for $d_c/d_{out} = 10$), d_{out} is the outer diameter and I is the bending inertia moment of the pipe. M_{PHP} is the pure bending moment of the coil-PHP (eq.1) and it is the defined by the following equation:

$$M_{PHP} = \frac{\theta \cdot E \cdot I}{L_c} \quad (3)$$

where θ is the deploying angle of the coil body (Fig.4), E is the Young's modulus of the material and L_c is the coil length ($L_c = \pi d_c N$, where d_c is the coil diameter and N is the number of the coils).

Therefore, to design a the spring shaped PHP six parameters should be accounted; four geometric parameters: the inner and outer pipe diameter (d_{in}/d_{out}), the number of coils (N) and the coil diameter (d_c), and lastly, two material properties: the yield stress (σ_y) and the Young's modulus (E) of the material. The inner diameter is here set to d_{in} = 1.8 mm, which is smaller than the capillary threshold at ambient temperature for most of the fluids (water, ethanol, methanol) usually employed for PHP devices. The above-mentioned parameters, are linked by the following equation, get by (eq.2) and (eq. 3):

$$\frac{\sigma_y}{E} = \frac{\theta}{\pi d_c N}\frac{d_{out}}{2} \tag{4}$$

Notice that the maximum coil stress must be equal to the yield stress of the pipe material corrected by the safety factor ($\sigma_y = SF \cdot \sigma_c^{max}$).

A preliminary selection of the materials respecting the mechanical criterion is performed on aluminium and copper alloys and the most suitable material is Al6063 ($E = 68$ GPa, $\sigma_y = 96$ MPa). In order to improve the mechanical properties, the aluminium tube is cold formed into the spring shape and it is subsequently tempered (160 ℃ for 8 hours) to increase the yield stress of the material up to 298 MPa . The moment needed for a 90 deg rotation of the panel get by eq.4 is 220 Nmm.

The results have been even validated by a Finite Element Method solver (ANSYS, Inc.) solving the spring mechanical problem in a dynamic 3D configuration.

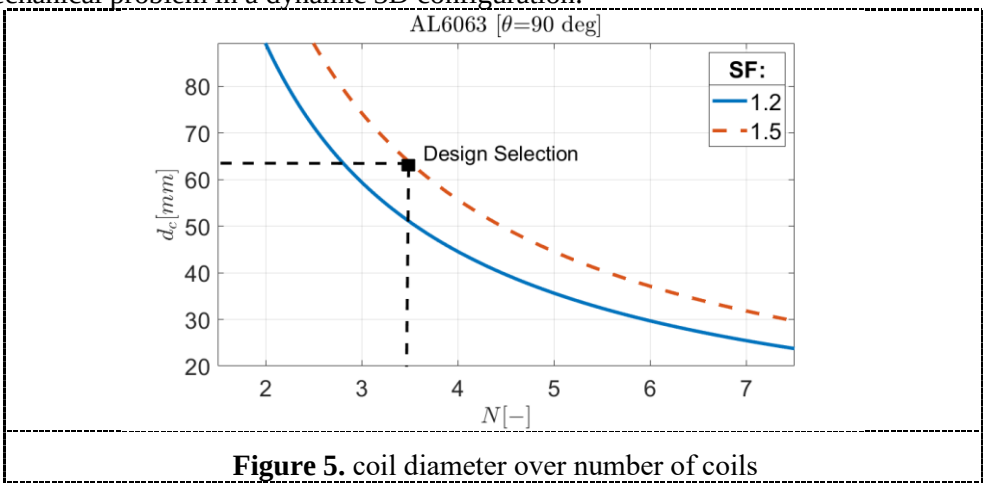

Figure 5. coil diameter over number of coils

Once the material has been selected, to complete the PHP torsional spring design the diameter and the number of the coil is chosen to respect the compactness constraint. Figure 5 shows the coil diameter as a function of the number of coils for two safety factor, SF = 1.2 (blue line) and SF = 1.5 (orange dashed line). Notice that as the coil diameter increases (d_c =20 up to 70 mm) the number of coils decreases (N = 7.5 down to 2. 5). Figure 6 shows the first prototype of a single adiabatic junction spring shaped with an aluminium pipe. The increase in the number of coils has two main effects: the increase of the device width and the increase of the distance between the fixed (evaporator section – Fig.6) and the moving part (condenser section – Fig.6) sections. Both of them results in a minor compactness (y-axis, Fig.6). Based on the design constraints of the ESA prototype and the above considerations, a good compromise is $d_c = 65$ mm and N = 3.5 for a SF=1.5.

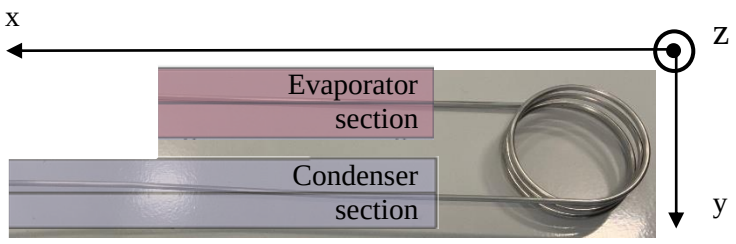

Figure 6. Aluminum tube bent into a spring to obtain a foldable Pulsating Heat Pipe tube portion.

3.2. Pressure Drops in helical pipe

Once the mechanical aspect of the spring-shaped Pulsating Heat Pipe has been performed, the thermo-fluidodynanic aspect must be considered. The helical shape of the adiabatic junction can affect the pressure drops in the capillary pipe and the performance of the whole two-phase passive system. The pressure losses in a helical shaped channel can be calculated according to the following equation [6]:

$$\Delta P_c = f_c \frac{\rho_l u_l^2}{2 d_{in}} L_l \tag{5}$$

where $L_l = (1-\alpha)\pi\, d_c N$ is the length of the liquid plug in the spring defined as a function of the void fraction (α), ρ_l and u_l are respectively the liquid density and velocity, d_{in} is the inner diameter and f_c is the friction factor due to the helical shape. The literature review mainly focuses on a laminar flow in helical capillary tubes and low coil factor ($d_{in}/d_c = 0.01 - 0.04$) (references from [6] to [14] listed in Table1.)

Table 1: Resume of the literature review.

	year	authors	d_{in} [mm]	d_c [cm]	d_{in}/d_c	working fluid	$\dot{m}$ [kg/h]
1	2006	Zhou et al. [6]	1-2.2	4-60	0.01-0.03	R22	50-60
2	2007	Valladares et al. [7]	1-1.6	4-20	0.01-0.03	R22	50-60
						R407c	50-60
						R410a	60-70
3	2010	Zhou et al. [8]	1.4;1.6	4	0.04	HCFC22	60
						HC290	30
4	2010	Chingulpitak et al. [9]	1-2.2	4-20	0.01-0.03	R407c	40-60
						R134a	50-70
						R22	40-60
5	2011	Agrawal et al. [8]	1-1.71	4-20	0.01-0.03	R22	50-60
6	2011	Chingulpitak et al. [11]	0.84-1.52	4-12	0.01-0.02	R22	20-50
						R134a	7-10
						R407c	10-40
7	2012	Wang et al. [12]	0.64	4	0.01-0.02	R22	10-50
8	2015	Deodhar et al. [13]	1.07	1-11.5	0.01-0.11	R134a	3-15
9	2017	Jadhav et al. [14]	1-1.8	4 - 20	0.01-0.03	R744	10-15

The Schmidt correlation [6] has been assumed by all the authors presented in Table 1 and therefore used in the present analysis. The friction factor is therefore described by the following equation:

$$f_c = f_s\left[1 + 0.14\,\mathrm{Re}^{\left(1-\frac{0.0644}{\left(\left(\frac{Re}{De}\right)^2\right)^{0.312}}\right)\Big/\left(\left(\frac{Re}{De}\right)^2\right)^{0.97}}\right] \tag{6}$$

where f_s is friction factor for straight capillary tube ($f_s = Re/64$ for laminar flow), Re and De are the Reynolds number and the Dean number respectively, expressed by the following equations:

$$Re = \frac{\rho_l u_l d_{in}}{\mu_l}; \qquad De = Re\sqrt{\frac{d_{in}}{d_c}} \tag{7}$$

where ρ_l, μ_l and u_l are density, dynamic viscosity and velocity of the liquid, respectively. Figure 7 shows the pressure drops (x-axis), as a function of coil diameter (y-right axis) and the Dean number (y-left axis) relative to water at 300 K, $u = 0.15$ m/s and void fraction $\alpha = 0$. The pressure drops increase as the coil diameter decreases and the coil number increases (Fig. 7). In the prototype, ($d_c = 65$ mm, N

= 3.5) the pressure drops are $\Delta P_c = 0.5$ kPa. Unfortunately, the correlations in the literature present application range far from the usual PHP operative condition (oscillating flow and low mass flow rate), so a further specific experimental activity must be carried out to understand their prediction accuracy.

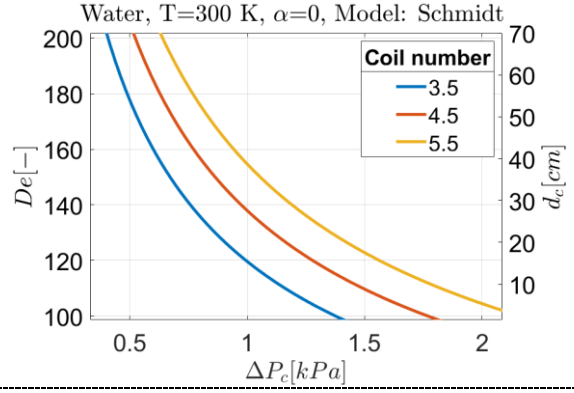

Figure 7. Pressure drops for a coiled adiabatic PHP a different Dean numbers

4. Shape Memory Alloy Actuator design

4.1. Shape memory effect and Brinson model

The shape memory effect (SME) is the ability of the material, after a residual mechanical deformation up to 5% [15], to recover its shape when the temperature is increased, thanks to the transition of the martensite/austenite crystal structure. The transition temperatures are the Austenite start/finish (A_s/A_f) and the Martensite start/finish (M_s/M_f) (Fig. 8). The thermomechanical behaviour of shape memory alloy can be predicted by the Brinson model [15]. The constitutive equation is based on the thermomechanical equilibrium in the material where the temperature T and the stress σ_{SMA} are constant along the material as follows:

$$\Delta\sigma_{SMA} = E \cdot \Delta\epsilon + \Delta\Omega + \Theta\Delta T \quad (8)$$

where ϵ is the strain while E is Young's modulus and varying with the martensite fraction. In addition, Ω is the deformation due to phase-transformation and Θ is the expansion thermal coefficient.

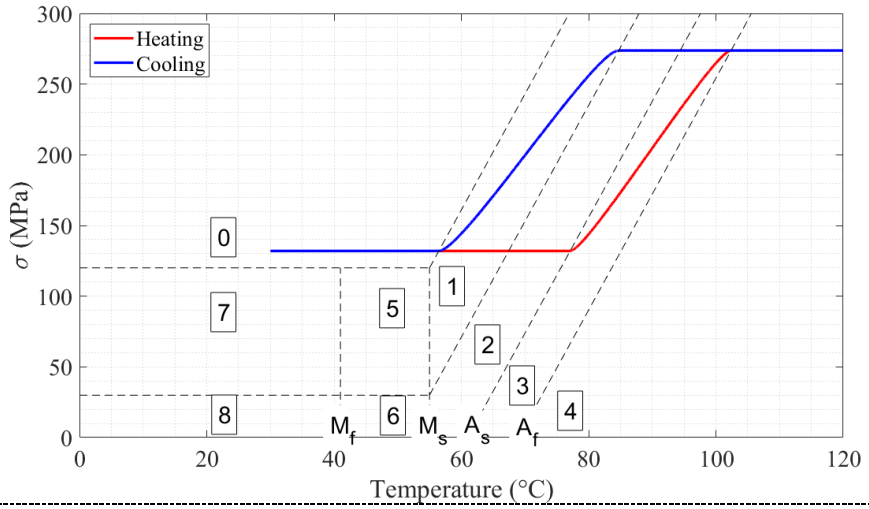

Figure 8. Uniform temperature model, heating and cooling processes: stress over temperature [16]

Figure 8 shows the material phase transition, from Martensite (zone 0) to Austenite (zone 4) or vice versa, as a function of stress and temperature during the SMA heating/cooling. The results are obtained from a monodimensional model designed in Matlab®, which is able to predict the behaviour of an SMA

wire subjected to a spatial temperature gradient [16]. Martensite (zone 0 - Fig. 8) is obtained after mechanical stretching of the wire by the tensile machine. Starting from zone 0, the SMA is heated (red line - Fig. 8) above A_f to reach zone 4 (Fig. 8). Above this temperature, the SMA regains its original shape (shortening of the wire) going back into the parent austenitic phase (Zona 4 - Fig. 8). The zones between 5 and 8, concern the mechanical deformation at room temperature, while zone 1 to 3 describe the phase transformation from martensite to austenite or viceversa. When the SMA wire shortens due to the shape memory effect (SME), it applies a force F_{SMA} (Section 2 - Fig.4) on the movable plate of the device defined as follows:

$$F_{SMA} = \sigma_{SMA} A_{SMA} \tag{9}$$

where A_{SMA} is the cross-section of the SMA wire.
In a previous work the authors implemented the Brinson model considering a temperature gradient along the wire and defining the stress as a function of the panel deploying angle [16]. In the present paper the authors attempt to validate the model by means of the experimental apparatus described below.

4.2. Experimental apparatus

The prototype of the deployable panel is equipped with a SMA wire, diameter 0.5 mm, length 165 mm, as shown in Figure 9. The actuator is a Nitinol® wire ($Ni_{50}Ti_{50}$ - 50 % Nickel, 50 % Titanium), which is commercially and readily available and has already been extensively studied. To investigate the Shape Memory Effect, in this set-up, the coiled-PHP tube portion is replaced by a spring with the same mechanical characteristics. The wire passes through two pulleys and its force is counter-acted by a torsion spring, which keeps the device closed.

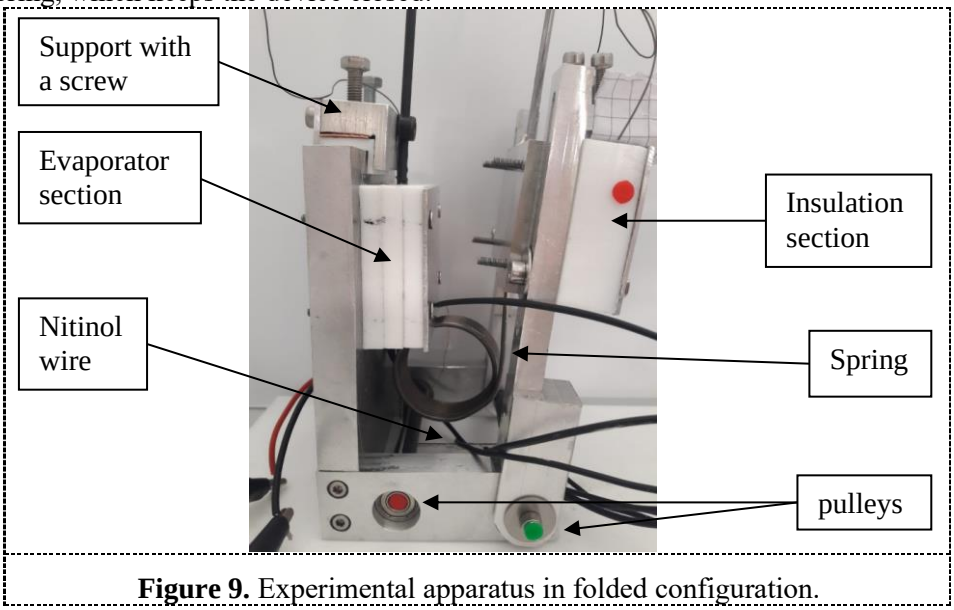

Figure 9. Experimental apparatus in folded configuration.

The wire is clamped between two PTFE blocks in the insulation section and between two copper elements in the evaporator section. Once the wire is heated, it shortens due to Shape Memory Effect (SME) and applies a force on the moving plate to deploy it. The wire is instrumented with seven T-type micro thermocouples (0.127 mm wire diameter, max error = ±0.3 °C). The first thermocouple is positioned inside the copper package (hot source), while the other six are positioned 15 mm from the previous one. The wire can be heated either by two different methods, joule effect and thermal conduction. A power supply unit (GW-Instek®, PSH-6006A, max error = ±3 W), controlled by a 0-10 V signal, sets the electrical potential of the set up. The electrical potential is supplied to the ends of the SMA wire (joule effect) and of a thermofoil heater (thermal conduction) produced by Minco® (model: HM6969). The controlling signal is calculated via a Proportional Integral Derivative (PID) algorithm having the ramp temperature T_r as a moving setpoint and the thermocouple temperature T_{TC} as measured value. A camera records the deploying of the insulation section and the rotation angle θ is measured by video recognition based on the red and green marks in Figure 9 (max error = ± 0.4 degrees). The austenite

starts transformation temperature $A_s = 65℃$ is measured experimentally by means of a Differential Scanning Calorimeter (DSC) and taken as reference point in the analysis.

4.3. Preliminary results

Two test cases are considered, depending on the heating strategy, i.e. active and passive (Tab. 2).
The maximum deploying angle of the panel in this configuration is $\theta_{joule} = 62$ deg and it has been reached under the Joule heating (Tab. 2). The panel unfolding is almost instantaneous, probably due to friction acting on the apparatus, during the test for a temperature between 106 °C and 162 °C. The tests, with a passive heating (heat conduction in the wire) are carried out with three different wire insulation conditions (Tab. 2). As shown in Table 2, the three wire insulation conditions are: without insulation (2), with a PTFE coating of the wire ($d_{ins} = 3$ mm) (3) and by filling all the empty volumes of the device envelope with aqueous foams (maximum insulation).

Table 2. Test Conditions and Results.

Heating	Test	Insulation	K [W/m K]	T_1 [°C]	T_2 [°C]	θ [deg]	comments
active	1	NO	-	120	120	62	-
passive	2	NO	-	120	41	1	-
	3	PTFE	0.2		46	2	Coating, $d_{ins} = 3$ mm
	4	Aqueous Foam	0.1		53	3.7	Filling empty volume of the device envelope
				145	55	6.5	

Figure 10 shows the temporal trend of the wire temperature and deploying angle for the Aqueous foam-insulated SMA wire. The limit due to the passive heating is represented by the temperature gradient along the wire. Notice that the SMA wire portion at temperature lower than A_s cannot recover the residual mechanical deformation. In this case the panel doesn't fully unfold.

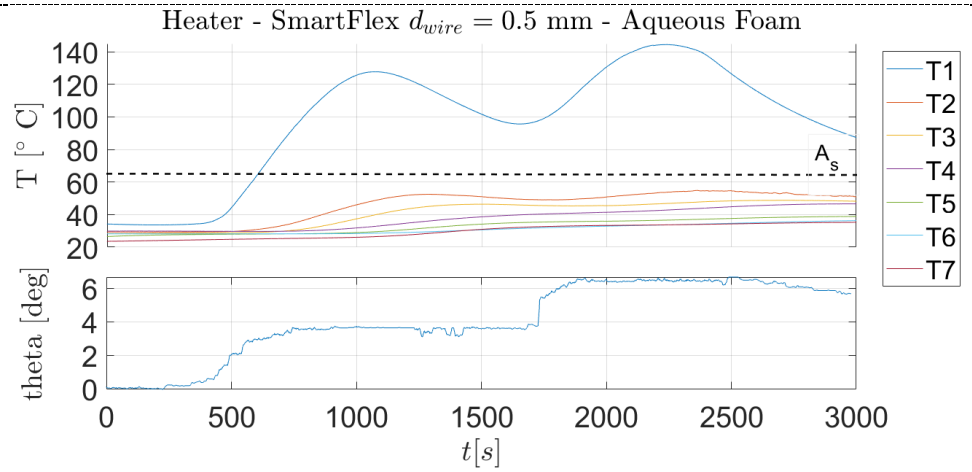

Figure 10. a) Temporal trend of the temperatures and Austenite start and b) Temporal trend of the deploying angle for the Aqueous foam-insulated SMA wire

Comparing the results (Tab.2), PTFE insulation with a diameter of $\mathbf{d_{ins} = 3\ mm}$ enhances the deploying by only 1 degree compared to the uninsulated case and the maximum temperature of the wire ($\mathbf{T_2}$) is **46** ℃. Advantages are obtained by filling all the empty volumes of the device envelope with aqueous foams. Indeed, as can be seen in Figure 10, the panel unfolds 3.7 degrees and the maximum wire temperature of **53** ℃ is reached (Tab.2). In this last test, the wire temperature at the evaporator section ($\mathbf{T_e^{max}}$) is increased up to **145** ℃, reaching a deploying angle of 6.5 degrees and a maximum temperature of the wire ($\mathbf{T_w^{max}}$) of **55** ℃.

5. Conclusions

The present work deals with the facilities study of a self-deployable Pulsating Heat Pipe actuated by Shape Memory Alloy. The Pulsating Heat Pipe is shaped as torsional spring in the adiabatic section and the device is unfolding by a SMA wire. The best performing material for the pulsating heat pipe is Al6063, heat treated (160 ℃ for 8 hours). A mock-up solution has been realized and successfully tested. A tool to design the coil shape and size for the PHP adiabatic section has been presented. It is based on the pressure losses prediction for helical capillary pipes, using the Schidmt's correlation. It has been highlighted as the plausible coil diameters could increase the pressure drops up to 8 times more than the actual solution. The SMA actuator is a Nickel-Titanium wire (SmartFlex® Wire). The foldable device should be passively actuated, and the experimental apparatus has been realized to verify the technical feasibility of the opening mechanism by using the single SMA wire in different configurations. Two test cases with a different heating strategy have been carried out: active (Joule effect) and passive (Heat conduction). In the case of Joule heating, the SMA wire is uniformly warmed up to the temperature of 120 ℃. The device considerably unfolds up to 62 degrees (maximum opening angle). In the case of passive heating three different solutions have been tested with different wire insulation conditions. In all the test has been noted that the temperatures along the wire are not constant and the wire portions undergoing the shape memory effect is small. For this reason, the achieved panel deployment is in the range 1-7 degrees, depending on the wire insulation. Under passive heating conditions, the panel unfolds by 10% compared to active heating. In conclusion, therefore, the solution of a single SMA-Nitinol wire is incompatible with the deploying of the passive system. In future works, wires in parallel and different SMA alloys with a conductivity higher than Nitinol will be evaluated to achieve the achievement.

Nomenclature

d	Diameter	[mm]	F	Force	[N]
$\dot{Q}$	Heat load	[W]	M	Bending moment	[Nmm]
T	Temperature	[℃]	ϵ	Strain	[-]
K	Bending stress correction factor	[-]	I	Bending inertia moment	[kg/m^2]
ΔP	Pressure drops	[kPa]	f	Friction factor	[-]
u	velocity	[m/s]	ρ	Density	[kg/m^3]
L	Length	[m]	α	Void fraction	[-]
ṁ	Mass flow rate	[kg/h]	μ	Dynamic viscosity	[Pa s]
Re	Reynold's number	[-]	De	Dean number	[-]
θ	Deploying angle	[deg]	Ω	deformation due to phase-transformation	[MPa]
σ	Stress	[MPa]	Θ	thermal coefficient of expansion	[MPa/℃]
E	Young's modulus	[GPa]	A	area	[m^2]

Subscripts

SMA	Shape Memory Alloy	PHP	Pulsating Heat Pipe
in	inner	out	outer
c	coil	N	Number of coil
y	yield	l	liquid
st	straight	e	evaporator
w	wire	max	maximum
A	Austenite	M	Martensite
exp	experimental	num	numerical
f	finish	s	start
r	ramp	TC	thermocouple

References

[1] G. Kiper and E. Söylemez, "Deployable space structures," in *RAST 2009 - Proceedings of 4th International Conference on Recent Advances Space Technologies*, 2009, pp. 131–138. doi: 10.1109/RAST.2009.5158183.

[2] M. J. Clifford and D. Eastwood, "Design of a novel passive solar tracker," *Solar Energy*, vol. 77, no. 3, pp. 269–280, Sep. 2004, doi: 10.1016/j.solener.2004.06.009.

[3] J. Qu, X. Li, Y. Cui, and Q. Wang, "Design and experimental study on a hybrid flexible oscillating heat pipe," *International Journal of Heat and Mass Transfer*, vol. 107, pp. 640–645, 2017, doi: 10.1016/j.ijheatmasstransfer.2016.11.076.

[4] E. Grossman and I. Gouzman, "Space environment effects on polymers in low earth orbit," in *Nuclear Instruments and Methods in Physics Research, Section B: Beam Interactions with Materials and Atoms*, Aug. 2003, vol. 208, no. 1–4, pp. 48–57. doi: 10.1016/S0168-583X(03)00640-2.

[5] J. S. R. Josephine Selvarani Ruth and K. Dhanalakshmi, "Shape memory alloy wire for self-sensing servo actuation," *Mechanical Systems and Signal Processing*, vol. 83, pp. 36–52, Jan. 2017, doi: 10.1016/j.ymssp.2016.05.042.

[6] G. Zhou and Y. Zhang, "Numerical and experimental investigations on the performance of coiled adiabatic capillary tubes," *Applied Thermal Engineering*, vol. 26, no. 11–12, pp. 1106–1114, Aug. 2006, doi: 10.1016/j.applthermaleng.2005.11.003.

[7] O. García-Valladares, "Numerical simulation and experimental validation of coiled adiabatic capillary tubes," *Applied Thermal Engineering*, vol. 27, no. 5–6, pp. 1062–1071, Apr. 2007, doi: 10.1016/j.applthermaleng.2006.07.034.

[8] G. Zhou, Y. Zhang, Y. Yang, and X. Wang, "Numerical model for matching of coiled adiabatic capillary tubes in a split air conditioner using HCFC22 and HC290," *Applied Thermal Engineering*, vol. 30, no. 11–12, pp. 1477–1487, Aug. 2010, doi: 10.1016/j.applthermaleng.2010.03.009.

[9] S. Chingulpitak and S. Wongwises, "Two-phase flow model of refrigerants flowing through helically coiled capillary tubes," *Applied Thermal Engineering*, vol. 30, no. 14–15, pp. 1927–1936, Oct. 2010, doi: 10.1016/j.applthermaleng.2010.04.026.

[10] N. Agrawal and S. Bhattacharyya, "Study of helically coiled adiabatic capillary tubes for transcritical CO2 expansion," *International Journal of Low-Carbon Technologies*, vol. 8, no. 4, pp. 245–252, Dec. 2013, doi: 10.1093/ijlct/cts047.

[11] S. Chingulpitak and S. Wongwises, "A comparison of flow characteristics of refrigerants flowing through adiabatic straight and helical capillary tubes," *International Communications in Heat and Mass Transfer*, vol. 38, no. 3, pp. 398–404, Mar. 2011, doi: 10.1016/j.icheatmasstransfer.2010.12.014.

[12] Q. Wang, Z. Rao, Y. Huo, and S. Wang, "Thermal performance of phase change material/oscillating heat pipe-based battery thermal management system," *International Journal of Thermal Sciences*, vol. 102, pp. 9–16, Apr. 2016, doi: 10.1016/j.ijthermalsci.2015.11.005.

[13] S. D. Deodhar, H. B. Kothadia, K. N. Iyer, and S. v. Prabhu, "Experimental and numerical studies of choked flow through adiabatic and diabatic capillary tubes," *Applied Thermal Engineering*, vol. 90, pp. 879–894, Nov. 2015, doi: 10.1016/j.applthermaleng.2015.07.073.

[14] P. Jadhav, N. Agrawal, and O. Patil, "Flow Characteristics of Helical Capillary Tube for Transcritical CO2 Refrigerant Flow," in *Energy Procedia*, Mar. 2017, vol. 109, pp. 431–438. doi: 10.1016/j.egypro.2017.03.055.

[15] L. C. Brinson, "One-dimensional constitutive behavior of shape memory alloys: Thermomechanical derivation with non-constant material functions and redefined martensite internal variable," *Journal of Intelligent Material Systems and Structures*, vol. 4, no. 2, pp. 229–242, 1993, doi: 10.1177/1045389X9300400213.

[16] A. Bacciotti, F. Bucchi, F. Frendo, M. Mameli, R. Perna, and S. Filippeschi, "On the use of shape memory alloys for deployable passive heat radiators in space satellites," *IOP Conference Series: Materials Science and Engineering*, vol. 1038, no. 1, p. 012061, Feb. 2021, doi: 10.1088/1757-899x/1038/1/012061.

Acknowledgments

The present work is carried forward in the framework of the ESAMAP Project entitled Two-phase passive thermal devices for deployable Space Systems (MAP Project number 4000128640). Thanks to Davide Della Vista, Enzo Peroni, Emanuele Del Gratta and Roberto Minelli for the technical contribution.